



Optimal strategies to steer and control water waves

Sebastiano Cominelli, Carlo Sinigaglia*, Davide Enrico Quadrelli, Francesco Braghin

Politecnico di Milano, Via Giuseppe La Masa, 1, Milano, 20156, Italy

ARTICLE INFO

Keywords:

Water waves
PDE-constrained optimization
Cloaking
Wind turbines

ABSTRACT

In this paper, we propose a new method for controlling surface water waves and their interaction with floating bodies. A floating target rigid body is surrounded by a control region where we design three control strategies of increasing complexity: an active strategy based on controlling the pressure at the air–water interface and two passive strategies where an additional controlled floating device is designed. Such device is modeled both as a membrane and as a thin plate and the effect of this modeling choice on the performance of the overall controlled system is analyzed. We frame this problem as an optimal control problem where the underlying state dynamics is represented by a system of coupled partial differential equations describing the interaction between the surface water waves and the floating target body in the frequency domain. An additional intermediate coupling is then added when considering the control floating device. The optimal control problem then aims at minimizing a cost functional which weights the unwanted motions of the floating body. A system of first-order necessary optimality conditions is derived and numerically solved using the finite element method. The efficacy of this new method for reducing hydrodynamic loads on floating objects has been shown through numerical simulations.

1. Introduction

Achieving control of how water waves interact with obstacles is a goal humankind has pursued from the very beginning of civilization, as witnessed by the early development of walls and breakwaters for coastal protection near harbors and cities on seashores. Recent technological advances related to the ever-increasing demand for renewable energy production have been accompanied by an increased interest in the installation of offshore wind farms and energy harvesting platforms aimed at turning undulatory motion into electrical energy. In the former case, the interaction between the waves and the floating platforms causes unwanted oscillations of the wind turbine, that in turn reduce the structural service life when not appropriately controlled (Adedipe et al., 2016). In the latter case, the capability of amplifying/focusing the oscillatory motion near the harvester could improve the overall performance. The classical approach to reduce the impact of water waves on offshore turbines is to employ active or passive control strategies (Kandasamy et al., 2016), mainly borrowing them from civil engineering, e.g., Tune Mass Dampers (TMD) (Zuo et al., 2020; Colwell and Basu, 2009; Jahangiri and Sun, 2020). A different route to achieve the same goal has developed during the last two decades inspired by the theory originally developed in (Leonhardt, 2006; Pendry et al., 2006) to achieve cloaking of electromagnetic waves. Such theoretical tool, called Transformation Theory (TT), unlocks the capability to compute a spatial distribution of inhomogeneous and

anisotropic material properties which modify how wave propagates in space (Kadic et al., 2016). Since then, similar techniques have been developed and adapted in a variety of different physical domains whose dynamical equations share a common mathematical structure, e.g. acoustics (Cummer and Schurig, 2007), elasticity (Norris and Shulov, 2011), heat conduction (Schittny et al., 2013), and water waves. Although the original goal of this research field was to make objects undetectable by field measurements by re-routing incident radiation around the obstacle and thus reducing scattering to zero (Farhat et al., 2008; Newman, 2014; Zhang et al., 2018, 2020; Porter and Newman, 2014; Zareei and Alam, 2015; Dupont et al., 2016), several works have applied the same idea with the different goal of preventing obstacle motion by minimizing interactions with the impinging wave, see, for example, (Alam, 2012; Zareei and Alam, 2016; Loukogeorgaki and Kashiwagi, 2019; Iida et al., 2023). In Alam (2012), it was proposed to modify the seabed shape for shielding floating objects from gravity waves, but in practical cases, like wind turbines or other plants, the installation of those objects mostly occurs in deep sea zones where the seabed shape is of little influence for wave propagation. Inspired by modeling techniques for floating ice in oceans (Keller and Goldstein, 1953; Fox and Squire, 1990), a more realistic device was theorized in Zareei and Alam (2016). It consists of a thin floating plate that surrounds a circular infinite cylinder in a constant depth environment

* Corresponding author.

E-mail address: sebastiano.cominelli@polimi.it (S. Cominelli).

and whose material properties are obtained by applying the conformal mapping method (Leonhardt, 2006). However, their solution is based on assumptions that should be relaxed in case of floating objects since the obstacle is assumed to be fixed and extended until the seabed. Furthermore, the designed material properties require the plate to be anisotropic and inhomogeneous, which may be difficult to manufacture in practice. Recently, Loukogeorgaki and Kashiwagi (2019) proposed to reduce the oscillations of a floating cylinder by optimizing the thickness of a homogeneous annular plate that floats around the cylinder; differently, Iida et al. (2023) considered a composite plate made of many concentric homogeneous layers. Both strategies are based on the analytical solution for axisymmetric floating objects.

In this paper, we follow another route and formulate an Optimal Control Problem (OCP) which allows us to take into account hydrodynamic interactions between water and a target floating body that does not extend to sea-bottom. The OCP formulation is also able to tackle arbitrary complex geometries and to include practical limits of the material properties as constraints. Furthermore, it is relatively straightforward to encode different objectives in the OCP formulation. As a result, this approach allows to design devices close to real-world applications. In setting the problem, control mechanisms that act on a region surrounding the obstacle are chosen; in particular, we investigate both active and passive control strategies that interact with the water surface.

The rigid-body motion of the floating structure can be measured by a cost function, so the problem is addressed as an Optimal Control Problem (OCP) constrained by a system of coupled Partial Differential Equations (PDEs) that govern the water and the control device dynamics.

In search of an optimal solution, we derive first-order necessary conditions by using a Lagrangian approach, see e.g. Manzoni et al. (2021), which are then solved by an iterative, gradient-based optimization algorithm for some relevant test cases.

A remarkable advantage of this approach is that problems of arbitrary geometries can be considered, which is of great importance in engineering applications. Moreover, similar to Cominelli et al. (2022), where a method for designing acoustic cloaks by solving PDE-constrained OCPs is proposed, we expect that a narrowband high-performance device will be achieved, and this is a good premise for applications involving swells, which are steady-state fully developed water waves generated by distant storms, and are characterized by narrowband spectra (Hasselmann et al., 1973).

A brief review of the paper organization follows. Section 2 describes the physical model adopted together with its main assumptions, then in Section 3 we propose an active control strategy that modifies the pressure on the air/water interface surrounding the floating target.

The resulting OCP is linear-quadratic and can be solved efficiently as a large linear system, additionally, fast-solving techniques are available for real-time applications, exploiting, for example, Model Order Reduction strategies (Sinigaglia et al., 2022). This control idea is well suited for floating systems such as Floating Production Storage and Offloading (FPSO), where energy can be spent for active control, conversely, this is hardly the case for floating turbines where a passive mechanism is sought instead.

After treating the active linear problem, passive strategies are considered in Sections 4 and 5. In particular, we analyze two control mechanisms that consist of covering a portion of the water surface around the turbine with a floating elastic membrane or a plate, respectively. The two models describing the coupled dynamics have been originally proposed for studying the effect of floating ice on water waves (Keller and Goldstein, 1953; Fox and Squire, 1990), and they now come in handy as constraints for the OCP.

In this case, the control is tuned by modifying stiffness and inertia properties of the floating device: by increasing the local stiffness, water waves experiment a speed up, conversely, they are slowed down as the inertia increases. Note that, differently from (Zareei and Alam, 2016), this framework guarantees the isotropy of both the membrane and the plate, as a consequence, we obtain a simpler device to manufacture.

2. Problem statement

Throughout this section, a brief summary of the main modeling equations applied for the rest of the paper is proposed; this turns out to be useful for Sections 3–5 in particular, where the different control actions considered lead to modifications of the system dynamics.

For a detailed derivation, the reader is referred to, e.g., the monograph by (Mei et al., 2005). The main assumptions are that the flow is inviscid, irrotational, and characterized by small wave amplitude.

Let us consider the volume of water $\Omega \subset \mathbb{R}^3$ depicted in Fig. 1 representing top and side views of a cylindrical portion of an ocean environment. Its disjoint boundaries are Γ_f , Γ_c , Γ_r , Γ_g and Γ_e . Γ_f and Γ_c are the free and the controlled parts of the air–water interface respectively, described by the time-varying surface $z = \zeta(x, y, t)$ and with equilibrium position $z = 0$; Γ_r is the sea bottom surface described by the function $h = h(x, y)$. Γ_g is the wetted surface of the target floating body and its position depends on the body motion; Γ_e is the artificial boundary introduced for computational reasons.

By assuming the variation in water density insignificant over the temporal and spatial scales of interest, the continuity and Navier–Stokes equations describing respectively the conservation laws of mass and momentum are :

$$\nabla \cdot \mathbf{u} = 0, \quad (1)$$

$$\mathbf{u}_t + \mathbf{u} \cdot \nabla \mathbf{u} = -\nabla \left(\frac{P}{\rho} + gz \right) + \nu \Delta \mathbf{u}, \quad (2)$$

inside the computational domain Ω , where $\mathbf{u} = \mathbf{u}(\mathbf{x}, t) \in \mathbb{R}^3$ is the velocity vector field and \mathbf{u}_t its partial time derivative while $\mathbf{u} \cdot \nabla \mathbf{u}$ denotes the convective terms using the classical fluid dynamics notation, i.e. $(\mathbf{u} \cdot \nabla \mathbf{u})_i = \sum_{j=1}^3 u_j \frac{\partial u_i}{\partial x_j}$. Furthermore, $P = P(\mathbf{x}, t)$ is the

pressure field, $\rho = 1030 \text{ kg m}^{-3}$ the water density, $g = 9.81 \text{ m s}^{-2}$ the gravitational acceleration, ν the kinematic viscosity coefficient; the vector $\mathbf{x} = (x, y, z)$ is referred with the z axis pointing vertically upward. Under the assumption of inviscid ($\nu = 0 \text{ m}^2 \text{ s}^{-1}$) irrotational flow, the velocity field can be expressed as the gradient of a scalar potential $\Phi(\mathbf{x}, t)$, see e.g. Mei et al. (2005)

$$\mathbf{u} = \nabla \Phi. \quad (3)$$

So, by merging Eq. (1) and Eq. (3), Φ must satisfy the Laplace equation

$$\Delta \Phi = 0. \quad (4)$$

Under the same assumptions, the well-known unsteady Bernoulli equation can be proved, starting from Eq. (1) and Eq. (2), obtaining $-\frac{P}{\rho} = gz + \Phi_t + \frac{1}{2} \|\nabla \Phi\|^2$. Finally, if the ratio $\varepsilon := 2\pi A/\lambda$ between the wave amplitude A and the wavelength λ is much smaller than one, that is $\varepsilon \ll 1$, the quadratic term can be neglected obtaining the linear relation

$$-\frac{P}{\rho} = gz + \Phi_t \quad \text{in } \Omega. \quad (5)$$

Throughout this paper, we develop control strategies that work indefinitely in time for systems characterized by specific frequencies, hence the frequency domain approach is adopted for reducing the computational effort in view of numerical solutions. Let us introduce the following variables:

$$\begin{pmatrix} \Phi(\mathbf{x}, t) \\ \zeta(x, y, t) \\ P(\mathbf{x}, t) \end{pmatrix} = \Re \left\{ \begin{pmatrix} \phi(\mathbf{x}) \\ \eta(x, y) \\ p(\mathbf{x}) \end{pmatrix} e^{j\omega t} \right\}. \quad (6)$$

where ϕ , η and p are complex valued functions and ω is the angular frequency. Thus, Eq. (4) and Eq. (5) become respectively

$$\Delta \phi = 0 \quad (7)$$

$$-\frac{P}{\rho} = gz + j\omega \phi. \quad (8)$$

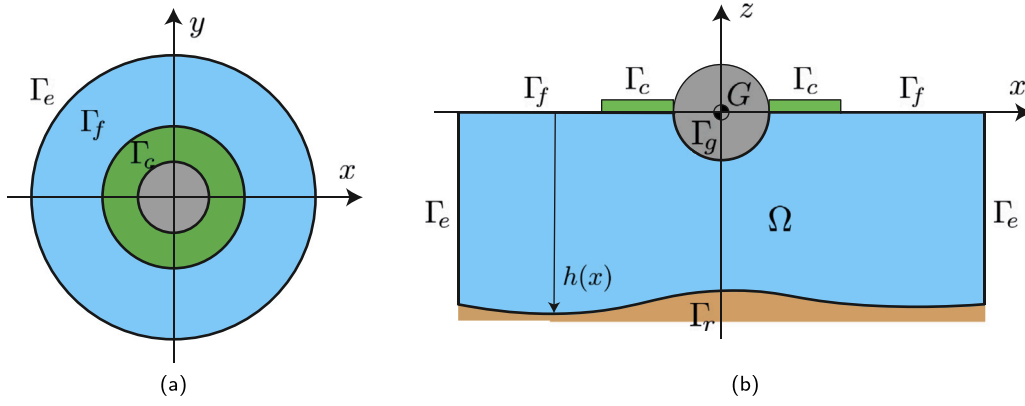


Fig. 1. Top (a) and side (b) views of the computational domain. The floating body is a sphere with a mass density equivalent to half than that of water. The green region represents the control surface.

2.1. Boundary conditions

We now briefly describe the remaining conditions that define a boundary value problem for the velocity potential ϕ . The seabed is considered as an infinitely rigid boundary; then, from Eq. (3), we can state that the velocity component normal to Γ_r is null, i.e.

$$\phi_n = 0 \quad \text{on } \Gamma_r, \quad (9)$$

where the subscript n stands for the derivative along the outgoing normal of the boundary.

Let us now consider the boundaries Γ_f and Γ_c : they belong to the surface $z = \zeta(x, y, t)$, whose shape depends both on space and time. However, under the assumption of small wave amplitude ($\varepsilon \ll 1$), it can be approximated up to the first order as the plane $z = 0$.

Using a first order expansion of the surface $z - \eta = 0$ and considering that $\varepsilon \ll 1$, one can obtain the following kinematic relationship

$$\phi_n = j\omega\eta \quad \text{on } \Gamma_f \cup \Gamma_c \quad (10)$$

that describes the continuity of velocity while neglecting the convective terms, see Mei et al. (2005) for a detailed derivation. In addition, on the air–water interface, the Bernoulli Eq. (5) states that

$$-\frac{p}{\rho} = g\eta + j\omega\phi \quad \text{on } \Gamma_f \cup \Gamma_c. \quad (11)$$

So, on the free surface Γ_f , the boundary condition on ϕ can be obtained by merging the last two expressions. Multiplying Eq. (11) by $j\omega$ and using Eq. (10), we obtain a boundary condition for ϕ on Γ_f :

$$g\phi_n - \omega^2\phi = -j\omega\frac{p}{\rho} \quad \text{on } \Gamma_f, \quad (12)$$

where the right-hand-side represents a forcing term coming from the environment, e.g. from wind. Conversely, the dynamics holding on the control surface Γ_c depends on the kind of control adopted. In this case, the kinematic relation (10) remains valid, while Eq. (11) changes according to the cases analyzed in Sections 3–5. We define an operator E which encodes the dynamic equilibrium that fluid velocity potential ϕ , vertical displacement η and control action u shall satisfy:

$$E(\phi, \eta, u) = 0 \quad \text{on } \Gamma_c. \quad (13)$$

For what concerns the wet surface of the floating body, Γ_g , two conditions have to be imposed: kinematic constraints on Γ_g and the balance of forces on the body. Even though the boundary moves following the motion of the body, up to the first order approximation it can be assumed fixed in its equilibrium position for solving in a simplified way the boundary value problem (Mei et al., 2005), such that the following two equations describing the linearized motion can be derived:

$$\phi_n = j\omega\{\mathbf{n}\}^T\{\mathbf{X}\} \quad \text{on } \Gamma_g \quad (14)$$

$$[K - \omega^2 M]\{\mathbf{X}\} = -j\omega\rho \int_{\Gamma_g} \phi\{\mathbf{n}\}d\Gamma + \{\mathbf{f}\} \quad (15)$$

where $\{\mathbf{X}\} = (\mathbf{x}^b, \boldsymbol{\theta}^b) \in \mathbb{C}^6$ is the column vector collecting the six degrees of freedom of the floating body in frequency domain: the three displacements $\mathbf{x}^b \in \mathbb{C}^3$ and the three rotation angles $\boldsymbol{\theta}^b \in \mathbb{C}^3$ of the body with respect to a fix point G ; $\{\mathbf{n}\} = (\mathbf{n}, (\mathbf{x} - \mathbf{x}_G) \times \mathbf{n})$, $\{\mathbf{n}\} : \mathbb{R}^3 \rightarrow \mathbb{R}^6$ is the generalized normal to the surface, with $\mathbf{n} = \mathbf{n}(\mathbf{x})$ the outgoing normal and \mathbf{x}_G the spatial coordinates of G . We indicate with \times the cross product between two vectors.

The vector $\{\mathbf{f}\} \in \mathbb{C}^6$ collects the external loads acting on the body and allows to consider the effect of forces due to wind and catenary mooring lines (Mei et al., 2005); for the sake of simplicity, we suppose $\{\mathbf{f}\} = \mathbf{0}$ for the rest of this paper. The floating body dynamics (15) depends on the stiffness and mass matrices K , $M \in \mathbb{R}^{6 \times 6}$ respectively, they are defined as:

$$K = \rho g \begin{bmatrix} 0 & 0 & 0 & 0 & 0 & 0 \\ 0 & 0 & 0 & 0 & 0 & 0 \\ 0 & 0 & \mathcal{A} & I_2^A & -I_1^A & 0 \\ 0 & 0 & I_2^A & I_{22}^A + I_3^V & -I_{12}^A & 0 \\ 0 & 0 & -I_1^A & -I_{21}^A & I_{11}^A + I_3^V & 0 \\ 0 & 0 & 0 & 0 & 0 & 0 \end{bmatrix}, \quad (16)$$

$$M = \begin{bmatrix} M^b & 0 & 0 & 0 & 0 & 0 \\ 0 & M^b & 0 & 0 & 0 & 0 \\ 0 & 0 & M^b & 0 & 0 & 0 \\ 0 & 0 & 0 & I_{22}^b + I_{33}^b & -I_{21}^b & -I_{31}^b \\ 0 & 0 & 0 & -I_{12}^b & I_{33}^b + I_{11}^b & -I_{32}^b \\ 0 & 0 & 0 & -I_{13}^b & -I_{32}^b & I_{11}^b + I_{22}^b \end{bmatrix},$$

where \mathcal{A} is the area of S^A , with S^A the cross-section of the body with respect to the plane $z = 0$, M^b the body mass, I^A and I^b are the first and second moments of inertia with respect of the surface S^A and the body volume V^b respectively, and I^V is the moments of inertia of the submersed volume V , i.e.:

$$I_i^A = \int_{S^A} (\mathbf{x} - \mathbf{x}_G)_i dS, \quad I_{ij}^A = \int_{S^A} (\mathbf{x} - \mathbf{x}_G)_i (\mathbf{x} - \mathbf{x}_G)_j dS, \\ I_i^V = \int_V (\mathbf{x} - \mathbf{x}_G)_i dV, \quad I_{ij}^b = \int_{V^b} (\mathbf{x} - \mathbf{x}_G)_i (\mathbf{x} - \mathbf{x}_G)_j dm. \quad (17)$$

For computational reasons, the domain has been truncated generating a fictitious cylindrical boundary Γ_e on which an absorbing condition must be imposed for avoiding artificial reflections. For the sake of simplicity, we consider a first order radiation condition (see e.g. Bai

(1972), Hsu et al. (2003), which is able to absorb waves with a small incidence angle on Γ_e with respect to the normal:

$$\phi_n^s + \alpha \phi^s = 0 \quad \text{on } \Gamma_e \quad (18)$$

where $\alpha = jk + \frac{1}{2R}$; ϕ^s is the scattered potential field with respect to the incident one ϕ^i , characterized by a single angular frequency ω and wavenumber k ; R is the base radius of the cylinder Γ_e . Note that since the floating obstacle is in the middle of the computational domain and the absorbing boundary is a cylinder surrounding the body, scattering is expected to come nearly orthogonal to Γ_e , thus leading to an acceptable numerical approximation for a computational domain sufficiently large relatively to the floating body and the control mechanism.

The incident field ϕ^i is the analytical solution of a wave propagating in a domain without obstacles and whose depth is constant, i.e. $h(x, y) \equiv h_0$:

$$\phi^i = j \frac{gA}{\omega} \frac{\cosh k(z + h_0)}{\cosh kh_0} e^{j\mathbf{k} \cdot \mathbf{x}}, \quad (19)$$

where \mathbf{k} is the wave vector and A is the wave amplitude. Wave number $k = |\mathbf{k}|$ and circular frequency ω must satisfy the dispersion relation $\omega^2 = gk \tanh kh_0$. In other words, Eq. (19) is the analytical solution to the potential Eq. (7), the free surface equilibrium (12) with $p = 0$ and the sea bed condition (9) in case there are no floating obstacles and the sea depth is constant and equal to h_0 . Again, the reader is referred to, e.g., Mei et al. (2005) for a detailed derivation.

The radiation condition (18) holds for the scattered field only, so we have to reformulate all the above equations in terms of ϕ^s making use of $\phi = \phi^s + \phi^i$, since ϕ is considered as the total velocity potential. We obtain the following linear elliptic PDE coupled with the rigid body dynamics and the pressure equilibrium on Γ_c :

$$\begin{cases} -\Delta \phi^s = 0 & \text{in } \Omega \\ \phi_n^s = 0 & \text{on } \Gamma_r \\ \phi_n^s - \frac{\omega^2}{g} \phi^s = 0 & \text{on } \Gamma_f \\ \phi_n^s = j\omega\eta - \phi_n^i & \text{on } \Gamma_c \\ \phi_n^s = j\omega\{\mathbf{n}\}^\top \{\mathbf{X}\} - \phi_n^i & \text{on } \Gamma_g \\ \phi_n^s + \alpha \phi^s = 0 & \text{on } \Gamma_e \end{cases} \quad (20)$$

$$(K - \omega^2 M)\{\mathbf{X}\} = -j\omega\rho \int_{\Gamma_g} (\phi^s + \phi^i)\{\mathbf{n}\} d\Gamma \quad (21)$$

$$E(\phi, \eta, u) = 0 \quad \text{on } \Gamma_c \quad (22)$$

Note that, for the sake of simplicity, the wind pressure on Γ_f is assumed to be null so the incoming wave is considered as generated away from the region of interest, that is a consistent hypothesis in case of swells. Also, the sea bed is considered of constant depth. In this setting, the scattered field ϕ^s includes the perturbation with respect to ϕ^i given by the floating body and due to any control action we apply.

3. Active pressure control

In this Section, we formulate and solve the active control problem where the surface pressure around the obstacle is considered as control mechanism. The control space is denoted by \mathcal{U} and it is selected as $L^\infty(\Gamma_c, \mathbb{C}) \cap H^1(\Gamma_c, \mathbb{C})$. The cost functional $J : \mathbb{C}^6 \times \mathcal{U} \rightarrow \mathbb{R}$ is defined as

$$J(\{\mathbf{X}\}, u) := \frac{1}{2} \{\mathbf{X}\}^\dagger C \{\mathbf{X}\} + \frac{1}{2} \|u\|_{\mathcal{U}}^2, \quad (23)$$

where $\{\mathbf{X}\}^\dagger = \{\bar{\mathbf{X}}\}^\top$ stands for the Hermitian of $\{\mathbf{X}\}$ and $C \in \mathbb{R}^{6 \times 6}$ is a positive definite weighting matrix; the norm $\|u\|_{\mathcal{U}}$ on the space \mathcal{U} is defined as the weighted norm

$$\|u\|_{\mathcal{U}}^2 := (\bar{u}, u)_{\mathcal{U}} = \alpha_u \|u\|_{L^2(\Gamma_c)}^2 + \beta_u \|\nabla u\|_{L^2(\Gamma_c)}^2, \quad (24)$$

where $\alpha_u, \beta_u > 0$ are regularization parameters that allow us to limit separately the control effort and the spatial control gradient respectively. In particular, α_u limits the control effort, while β_u imposes a soft constraint on the control gradient.

Note that the cost functional involved in the OCP is the same independently on the control mechanism since, through all the paper, the aim is to control the water flow such that the floating body motion is minimized.

The first scenario here considered is that of an active source applying a pressure field on the boundary Γ_c , surrounding the floating body. An exact solution can be obtained in this case without any iterative algorithm, due to the linear-quadratic nature of the problem. This fact makes the following discussion appealing for real-time applications, e.g. for Linear Quadratic Regulators (Manzoni et al., 2021).

Hence, the unknown is the surface pressure $p|_{\Gamma_c} = u$, $u : \mathbb{R}^2 \rightarrow \mathbb{C}$ such that the cost functional J is minimized. Since the only action on the surface Γ_c is a pressure, the condition $E(\phi, \eta, u) = 0$ can be obtained by the Bernoulli Eq. (5) evaluated on Γ_c :

$$E(\phi, \eta, u) = g\eta + j\omega\phi + \frac{u}{\rho}. \quad (25)$$

It can be merged with the kinematic relation (10) to obtain $\phi_n - \frac{\omega^2}{g} \phi = -j\frac{\omega}{\rho g} u$, on Γ_c and

$$\phi_n^s - \frac{\omega^2}{g} \phi^s = -j\frac{\omega}{\rho g} u \quad \text{on } \Gamma_c \quad (26)$$

since $\phi_n^i - \frac{\omega^2}{g} \phi^i = 0$ on Γ_c . Then the OCP reads

$$\begin{aligned} \min_{u \in \mathcal{U}_{ad}} \tilde{J} &= J(\{\mathbf{X}\}(u), u) \\ \text{s.t.} \quad &\begin{cases} -\Delta \phi^s = 0 & \text{in } \Omega \\ \phi_n^s = 0 & \text{on } \Gamma_r \\ \phi_n^s - \frac{\omega^2}{g} \phi^s = 0 & \text{on } \Gamma_f \\ \phi_n^s - \frac{\omega^2}{g} \phi^s = -j\frac{\omega}{\rho g} u & \text{on } \Gamma_c \\ \phi_n^s = j\omega\{\mathbf{n}\}^\top \{\mathbf{X}\} - \phi_n^i & \text{on } \Gamma_g \\ \phi_n^s + \alpha \phi^s = 0 & \text{on } \Gamma_e \end{cases} \\ &(K - \omega^2 M)\{\mathbf{X}\} = -j\omega\rho \int_{\Gamma_g} (\phi^s + \phi^i)\{\mathbf{n}\} d\Gamma \end{aligned} \quad (27)$$

For the sake of simplicity, we choose $\mathcal{U}_{ad} = \mathcal{U}$, and so the existence and uniqueness of a solution is guaranteed since α_u, β_u are strictly positive (Manzoni et al., 2021). By adopting a Lagrange multiplier method, a system of first-order necessary conditions is derived; see, e.g. Manzoni et al. (2021). We define the Lagrangian $\mathcal{L} : \mathcal{W} \times \mathcal{W}' \times \mathbb{C}^6 \times \mathbb{C}^6 \times \mathcal{U} \rightarrow \mathbb{R}$ as

$$\begin{aligned} \mathcal{L} = J + \Re \Big\{ &\int_{\Omega} \nabla \bar{\lambda} \cdot \nabla \phi^s - \frac{\omega^2}{g} \int_{\Gamma_f} \bar{\lambda} \phi^s - \frac{\omega^2}{g} \int_{\Gamma_c} \bar{\lambda} \phi^s + j \frac{\omega}{\rho g} \int_{\Gamma_c} \bar{\lambda} u \\ &- j\omega \int_{\Gamma_g} \bar{\lambda} \{\mathbf{n}\}^\dagger \{\mathbf{X}\} + \int_{\Gamma_g} \bar{\lambda} \phi_n^i + \alpha \int_{\Gamma_e} \bar{\lambda} \phi^s + \{\mathbf{Y}\}^\dagger \left[(K - \omega^2 M)\{\mathbf{X}\} \right. \\ &\left. + j\omega\rho \int_{\Gamma_g} (\phi^s + \phi^i)\{\mathbf{n}\} d\Gamma \right] \Big\}. \end{aligned} \quad (28)$$

where $\lambda \in \mathcal{W}'$ is the adjoint of the state ϕ^s and $\mathcal{W}' = H^1(\Omega, \mathbb{C})$ its functional space, $\{\mathbf{Y}\} \in \mathbb{C}^6$ the adjoint of $\{\mathbf{X}\}$. With a slight abuse of notation, we omit the differentials inside integrals. Note that the real part of the scalar products is taken, but similar results can be obtained by considering the imaginary part instead.

By taking the Gateaux derivative of \mathcal{L} with respect to the state ϕ^s , the derivative with respect to $\{\mathbf{X}\}$, and by requiring they are null, the optimality conditions on the adjoints state that:

$$\mathcal{L}'_{\phi^s}[\varphi] = \frac{1}{2} \left\{ \int_{\Omega} \nabla \bar{\lambda} \cdot \nabla \varphi - \frac{\omega^2}{g} \int_{\Gamma_f \cup \Gamma_c} \bar{\lambda} \varphi + \alpha \int_{\Gamma_e} \bar{\lambda} \varphi + j\omega\rho \{\mathbf{Y}\}^\dagger \int_{\Gamma_g} \varphi \{\mathbf{n}\} d\Gamma \right\} = 0 \quad \forall \varphi \in \mathcal{W}, \quad (29)$$

$$\mathcal{L}'_{\{X\}} = \frac{1}{2} \{X\}^\dagger C + \frac{1}{2} \left\{ -j\omega \int_{\Gamma_g} \bar{\lambda} \{n\}^\dagger + \{Y\}^\dagger (K - \omega^2 M) \right\} = 0, \quad (30)$$

where Wirtinger's calculus rules have been applied for handling complex derivatives (Wirtinger, 1927). The respective strong formulations are:

$$\begin{cases} -\Delta \lambda = 0 & \text{in } \omega \\ \lambda_n = 0 & \text{on } \Gamma_r \\ \lambda_n - \frac{\omega^2}{g} \lambda = 0 & \text{on } \Gamma_f \cup \Gamma_c \\ \lambda_n = j\omega \rho \{n\}^\top \{Y\} & \text{on } \Gamma_g \\ \lambda_n + \bar{\alpha} \lambda = 0 & \text{on } \Gamma_e \end{cases} \quad (31)$$

$$(K - \omega^2 M)^\top \{Y\} = -j\omega \int_{\Gamma_g} \lambda \{n\} d\Gamma - C^\top \{X\}$$

Finally, the reduced cost gradient is obtained by taking the derivative of Eq. (28) with respect to u :

$$\mathcal{L}'_u[\psi] = \int_{\Gamma_c} \left(\frac{\alpha_u}{2} \bar{u} \psi + \frac{\beta_u}{2} \nabla \bar{u} \cdot \nabla \psi + j \frac{\omega}{2\rho g} \bar{\lambda} \psi \right) d\Gamma = 0 \quad \forall \psi \in \mathcal{U}_{ad}; \quad (32)$$

note that the equality holds since $\mathcal{U}_{ad} = \mathcal{U}$.

In search of a numerical solution, we rely on a Galerkin \mathbb{P}_2 Finite Element Method (FEM) for discretizing the optimization problem. Thus a triangulation \mathcal{T}_h of Ω with characteristic size $h > 0$ is considered and the discrete spaces \mathcal{W}_h and \mathcal{W}'_h of \mathcal{W} and \mathcal{W}' are defined respectively; accordingly, \mathcal{U}_h is the discrete control space defined on the discrete counterpart of Γ_c . As a consequence, state, adjoint, and control are discretized as

$$\phi^s(\mathbf{x}) \approx \varphi(\mathbf{x})^\top \boldsymbol{\phi}, \quad \lambda(\mathbf{x}) \approx \varphi(\mathbf{x})^\top \boldsymbol{\lambda}, \quad u(\mathbf{x}) \approx \psi(\mathbf{x})^\top \mathbf{u}, \quad (33)$$

The discrete cost functional and the optimality necessary conditions are

$$\text{Cost functional:} \quad J = \frac{1}{2} \{X\}^\dagger C \{X\} + \frac{\alpha_u}{2} \mathbf{u}^\dagger E_c \mathbf{u} + \frac{\beta_u}{2} \mathbf{u}^\dagger A_c \mathbf{u} \quad (34)$$

$$\begin{aligned} \text{State:} \quad & \left[A - \frac{\omega^2}{g} (C_f + C_c) + \alpha C_e \right] \boldsymbol{\phi} = j\omega K_g^\top \{X\} \\ & + \mathbf{f}_g - j \frac{\omega}{\rho g} D_c \mathbf{u} \\ & (K - \omega^2 M) \{X\} = -j\omega \rho (K_g \boldsymbol{\phi} + \mathbf{g}) \end{aligned} \quad (35)$$

$$\begin{aligned} \text{Adjoint state:} \quad & \left[A - \frac{\omega^2}{g} (C_f + C_c) + \bar{\alpha} C_e \right] \boldsymbol{\lambda} = j\omega \rho K_g^\top \{Y\} \\ & (K - \omega^2 M) \{Y\} = -j\omega K_g \boldsymbol{\lambda} - C^\top \{X\} \end{aligned} \quad (36)$$

$$\text{Control gradient:} \quad \nabla_{\mathbf{u}} J = \left(\frac{\alpha_u}{2} E_c + \frac{\beta_u}{2} A_c \right) \bar{\mathbf{u}} + j \frac{\omega}{2\rho g} D_c^\top \bar{\boldsymbol{\lambda}} = \mathbf{0} \quad (37)$$

where $A \in \mathbb{R}^{n \times n}$ is the stiffness matrix on the domain Ω ; C_f , C_c and $C_e \in \mathbb{R}^{n \times n}$ are the mass matrices on the boundaries Γ_f , Γ_c and Γ_e respectively. $D_c \in \mathbb{R}^{n \times l}$ is the control matrix and $A_c, E_c \in \mathbb{R}^{l \times l}$ are the stiffness and the mass matrices in Γ_c . The matrix $K_g \in \mathbb{R}^{6 \times n}$ is defined as

$$(K_g)_{ij} := \int_{\Gamma_g} \{n\}_i \varphi_j d\Gamma; \quad (38)$$

$\mathbf{f}_g \in \mathbb{C}^n$ and $\mathbf{g} \in \mathbb{C}^6$ are forcing terms given by the background field, i.e.

$$\mathbf{f}_g = \int_{\Gamma_g} -\phi_n^i \boldsymbol{\varphi} d\Gamma \quad \mathbf{g} = \int_{\Gamma_g} \phi^i \{n\} d\Gamma \quad (39)$$

The OCP (27) is a linear quadratic one, as a consequence, it is also convex given that the weighting matrices in the cost functional are positive definite (Manzoni et al., 2021) and the necessary conditions are also sufficient; then its global minimum can be obtained by solving

the following linear system

$$\begin{bmatrix} A_{tot} & -j\omega K_g^\top & \mathbf{0} & \mathbf{0} & j \frac{\omega}{\rho g} D_c \\ j\omega \rho K_g & (K - \omega^2 M) & \mathbf{0} & \mathbf{0} & \mathbf{0} \\ \mathbf{0} & \mathbf{0} & A_{tot}^\dagger & -j\omega \rho K_g^\top & \mathbf{0} \\ \mathbf{0} & C^\top & j\omega K_g & (K - \omega^2 M) & \mathbf{0} \\ \mathbf{0} & \mathbf{0} & -j \frac{\omega}{2\rho g} D_c^\top & \mathbf{0} & \frac{\alpha_u}{2} E_c + \frac{\beta_u}{2} A_c \end{bmatrix} \begin{pmatrix} \boldsymbol{\phi} \\ \{X\} \\ \boldsymbol{\lambda} \\ \{Y\} \\ \mathbf{u} \end{pmatrix} = \begin{pmatrix} \mathbf{f}_g \\ j\omega \rho \mathbf{g} \\ \mathbf{0} \\ \mathbf{0} \\ \mathbf{0} \end{pmatrix}, \quad (40)$$

where $A_{tot} = A - \frac{\omega^2}{g} (C_f + C_c) + \alpha C_e$.

As a case study, we consider a floating sphere with homogeneous density $\rho_b = 0.5\rho$ such that, in the static equilibrium condition, the body is half submerged as shown in Fig. 1. The center of mass is assumed to be in the origin, i.e. $\mathbf{x}_G = \mathbf{0}$. Due to the spherical symmetry, the only non-null term of the K matrix is $(K)_{33}$. This, in turn, implies that the interaction with water cannot result in a rotation of the body, since $(\mathbf{x} - \mathbf{x}_G) \times \mathbf{n} = \mathbf{0}$ on Γ_g and water viscosity is considered null. Since the dynamics is linear, a unitary wave amplitude of the incident wave in Eq. (19) is assumed for the sake of simplicity. We choose a flat seabed 2.5 m deep, i.e. $h(\mathbf{x}) = 2.5$ m, and the computational domain is limited to a cylinder of radius 4 m. The control surface is an annular region surrounding the sphere whose external radius is 1 m long.

The excitation wave period is set to $T = 1.2$ s such that the normalized wavelength $\lambda \approx 2.25$ m results in a relevant excitation of the floating body. Note that, since the aim is not to cloak the floating obstacle in the usual sense, the wavelengths of interest are very different from the ones considered in usual cloaking problems; in particular, a very short λ results in a small excitation of the target since the mean pressure on Γ_g is negligible. Conversely, a wave characterized by a relatively long wavelength push on the floating body coherently. The wave is assumed to propagate along the y -axis, i.e. $\mathbf{k} = (0, k, 0)$. Finally, we choose the cost C to be the diagonal matrix $C = \text{diag}(1, 1, 1, H^2, H^2, H^2)$, where $H = 1$ m is the characteristic height of the floating object. Finally, the regularization parameters are chosen as $\alpha_u = \beta_u = 1 \times 10^{-10}$.

The numerical problem is implemented in Matlab[®] thanks to the open source library redbKIT (Negri, 2016; Cominelli et al., 2022; Sinigaglia et al., 2022) and the OCP is solved by inverting the linear system (40). The optimal control action is shown in Fig. 2(a) and (b); due to the linearity of the problem, the reduction in oscillation is proportional to the control effort, which is limited only by the weight α in the cost definition (23). According to how the mechanism will be realized, the control effort can be limited by either changing α or adding constraints on the space \mathcal{U} . Table 1 shows the motion amplitudes in terms of amplitude and phase of $\{X\}$. It is clear that this strategy reduces noticeably the oscillations of the floating sphere.

4. Surface tension and floating mass

In case energy availability is limited, relying on a passive strategy is a reasonable alternative. However, while active controls can easily modify the wave propagation by acting as sources, a passive strategy usually relies on steering waves by locally modifying the wave speed. The latter approach is analyzed in the following, where we design a floating device whose inertia and stiffness properties allow the symmetric control on wave speed we need.

Floating membrane dynamics has been used as a simplified model for floating ice and was proposed by Keller and Goldstein (1953) where the effect of inertia and surface tension on the propagation of water

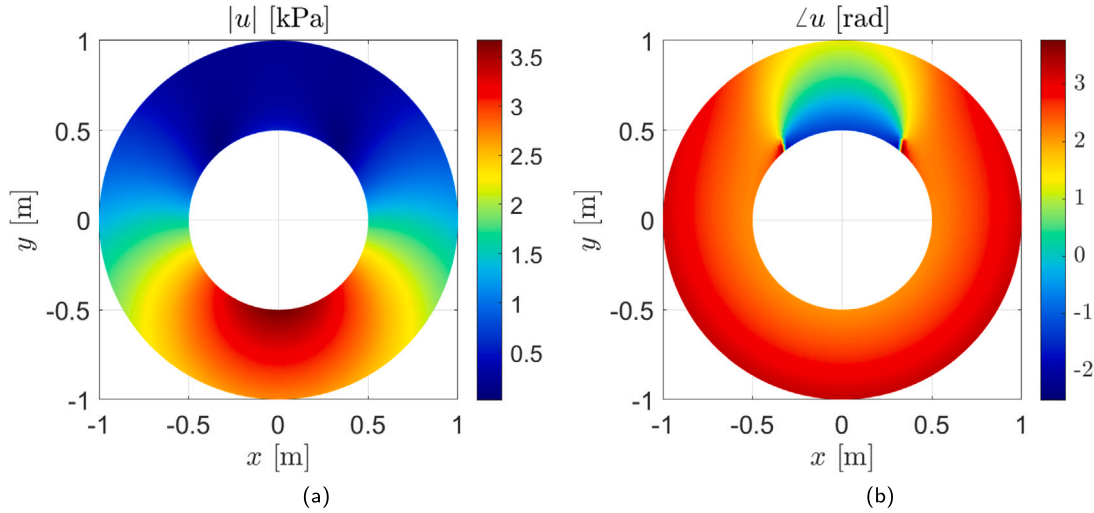


Fig. 2. Amplitude (a) and phase (b) of the optimal pressure on Γ_c ; the improvement of the oscillations $\{\mathbf{X}\}$ is summarized in Table 1. The control action is mainly distributed on the obstacle side facing the wave and, for the most part, has a phase of π , that indicates phase opposition with respect to the incoming wave; in this way, the wave is reflected before it interacts with the obstacle.

Table 1

Comparison between body motion in case of the three different control strategies; the values describing rotations are not reported because, thanks to the symmetries of the sphere, they are almost zero and derive from numerical errors only. These results highlight that the active control strategy is the most effective and the performance of the floating membrane is better than the floating plate. However, this trend is opposite to the feasibility of the strategies, so a compromise is needed.

$\{\mathbf{X}\}$ [$1 \angle \text{rad}$]	Uncontrolled	Pressure-controlled	Membrane-controlled	Plate-controlled
x	0.000 \angle -2.19	0.000 \angle -1.99	0.000 \angle -1.33	0.002 \angle -1.30
y	0.365 \angle -1.37	0.014 \angle -1.37	0.196 \angle -0.11	0.572 \angle -0.72
z	1.539 \angle -2.99	0.003 \angle -2.98	0.131 \angle -3.0	0.102 \angle -0.35
J	1.25	6.54×10^{-3}	7.05×10^{-2}	2.08×10^{-1}
$\frac{1}{2} \{\mathbf{X}\}^\top C \{\mathbf{X}\}$	1.25	1.07×10^{-4}	3.49×10^{-2}	1.16×10^{-1}

waves are considered. In particular, the loaded surface dynamics is derived by coupling the water flow with the motion of a membrane that is assumed to float on the surface, hence the vertical motion ζ of the water surface is assumed to be the same as the membrane displacement:

$$\nabla \cdot (T \nabla \zeta) = g \rho \zeta + \rho \Phi_t + m \zeta_{tt} + mg \quad \text{in } \Gamma_c, \quad (41)$$

where $T, m: \Gamma_c \rightarrow \mathbb{R}$ are the space varying surface tension and surface mass inertia, respectively. The left hand side accounts for the elastic restoring force, while the right hand side is the sum of the hydrostatic and hydrodynamic pressures, the inertia of the floating membrane, and its static load. We assume that the device cannot detach from the water surface; by virtue of this, the internal forces of the membrane can be modeled as an equivalent surface tension.

The constant gravity force mg causes a static displacement so it can be ignored while moving to the frequency domain:

$$\nabla \cdot (T \nabla \eta) = (g \rho - \omega^2 m) \eta + j \omega \rho \phi \quad \text{in } \Gamma_c, \quad (42)$$

According to this setup, the equilibrium function is $E = E(\phi, \eta, T, m)$ and takes the form of an elliptic PDE whose domain is the surface Γ_c . In the following, we control the dynamics Eq. (42) along with Eq. and Eq. (21) by acting on the control functions T and m .

For a complete definition of the state η , we need to impose also appropriate boundary conditions on $\partial \Gamma_c$. Since the membrane border is subject to a null shear force, it is free to oscillate and a homogeneous Neumann condition holds:

$$\eta_n = 0 \quad \text{on } \partial \Gamma_c. \quad (43)$$

Please note that this model assumes a horizontal equilibrium on the membrane boundary $\partial \Gamma_c$ which is hardly achievable in reality because

no external forces act on it; in addition, the internal equilibrium of the surface must be guaranteed even if T is space dependent.

We now define two control functions $u \in \mathcal{U}_{ad}$ and $v \in \mathcal{V}_{ad}$ that act on T and m such that

$$T = u, \quad 1 - \frac{\omega^2 m}{g \rho} = v. \quad (44)$$

u and v are constrained since T and m are positive and m must be upper limited for guaranteeing the buoyancy of the membrane. This second constraint depends on the density of the control device ρ_c and its thickness δ according to the formula $m = \rho_c \delta$, thus, in theory, no surface mass density m can prevent the membrane to float if a proper thickness is chosen. However, we assume the limiting case to be $\omega^2 m = g \rho$, which corresponds to the resonance condition of a floating object of surface mass m ; more loaded surfaces experience a vanishing of waves (Keller and Goldstein, 1953). Then, we define the admissible control spaces as:

$$\begin{aligned} \mathcal{U}_{ad} &= \{u \in \mathcal{U}, \varepsilon \leq u(\mathbf{x}) \quad \forall \mathbf{x} \in \Gamma_c\}, \\ \mathcal{V}_{ad} &= \{v \in \mathcal{V}, \varepsilon \leq v(\mathbf{x}) \leq 1 - \varepsilon \quad \forall \mathbf{x} \in \Gamma_c\}, \end{aligned} \quad (45)$$

where ε is chosen to be 1×10^{-6} to avoid numerical issues in case of null control actions.

Note that in this case $\mathcal{U} = H^1(\Gamma_c, \mathbb{R}) \cap L^\infty(\Gamma_c, \mathbb{R})$ is a space of real-valued functions, normed by the measure $\|u\|_T^2 = \int_{\Gamma_c} \alpha_u u^2 + \beta_u |\nabla u|^2 d\Gamma$, and that $\mathcal{U}_{ad}, \mathcal{V}_{ad}$ are convex sets.

Since there are two control actions, we redefine J as

$$J(\{\mathbf{X}\}, u, v) := \frac{1}{2} \{\mathbf{X}\}^\top C \{\mathbf{X}\} + \frac{1}{2} \|u\|_T^2 + \frac{1}{2} \|v\|_V^2. \quad (46)$$

Summing up, we aim at minimizing Eq. (46) such that the three coupled dynamics, (21) and (42) with Eq. (43) are satisfied, with $u \in \mathcal{U}_{ad}, v \in \mathcal{V}_{ad}$. Adopting the same strategy as before, we define

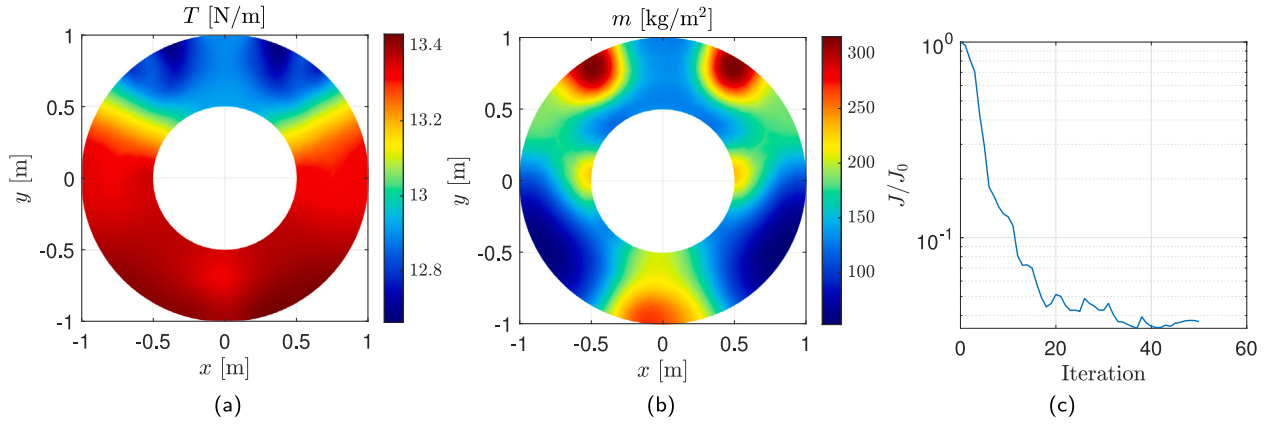


Fig. 3. Membrane properties given by the optimal control: surface tension T (a) and surface mass density m (b); objective over iteration (c). The improvement of the oscillations $\{\mathbf{X}\}$ is summarized in Table 1. The membrane stiffness is almost constant through the entire surface, so its role is mainly to speed up waves around the sphere and not to steer them. Conversely, the mass of the membrane concentrates mainly in three regions, this suggests that waves are steered mainly by inertia.

the Lagrangian $\mathcal{M} : \mathcal{W} \times \mathcal{W}' \times \mathbb{C}^6 \times \mathbb{C}^6 \times \mathcal{Y} \times \mathcal{Y}' \times \mathcal{U} \times \mathcal{U}' \rightarrow \mathbb{R}$ as

$$\begin{aligned} \mathcal{M}(\phi^s, \lambda, \{\mathbf{X}\}, \{\mathbf{Y}\}, \eta, \mu, u, v) := & J + \Re \left\{ \int_{\Omega} \nabla \bar{\lambda} \cdot \nabla \phi^s \right. \\ & - \frac{\omega^2}{g} \int_{\Gamma_f} \bar{\lambda} \phi^s + \int_{\Gamma_c} \bar{\lambda} (\phi_n^i - j\omega\eta) \\ & - j\omega \int_{\Gamma_g} \bar{\lambda} \{\mathbf{n}\}^\dagger \{\mathbf{X}\} + \int_{\Gamma_g} \bar{\lambda} \phi_n^i + \alpha \int_{\Gamma_e} \bar{\lambda} \phi^s \\ & + \{\mathbf{Y}\}^\dagger \left[(K - \omega^2 M) \{\mathbf{X}\} + j\omega \rho \int_{\Gamma_g} (\phi^s + \phi^i) \{\mathbf{n}\} \right] \\ & \left. + \int_{\Gamma_c} u \nabla \bar{\mu} \cdot \nabla \eta + g \rho v \bar{\mu} \eta + j\omega \rho \bar{\mu} (\phi^s + \phi^i) \right\}, \end{aligned} \quad (47)$$

where $\eta \in \mathcal{Y}$, $\mathcal{Y} = H^1(\Gamma_c)$, and $\mu \in \mathcal{Y}'$ the adjoint state of η , \mathcal{Y}' its adjoint space. The first order necessary conditions are obtained by taking the derivatives of \mathcal{M} with respect to the states ϕ^s , η and $\{\mathbf{X}\}$ and controls u , v . For the sake of brevity, the strong formulations are reported only:

$$\begin{aligned} \text{Adjoint:} \quad & \begin{cases} -\Delta \lambda = 0 & \text{in } \omega \\ \lambda_n = 0 & \text{on } \Gamma_r \\ \lambda_n - \frac{\omega^2}{g} \lambda = 0 & \text{on } \Gamma_f \\ \lambda_n = j\omega \rho \mu & \text{on } \Gamma_c \\ \lambda_n = j\omega \rho \{\mathbf{n}\}^\dagger \{\mathbf{Y}\} & \text{on } \Gamma_g \\ \lambda_n + \bar{\alpha} \lambda = 0 & \text{on } \Gamma_e \end{cases} \\ & (K - \omega^2 M)^\top \{\mathbf{Y}\} = -j\omega \int_{\Gamma_g} \lambda \{\mathbf{n}\} - C^\top \{\mathbf{X}\} \\ & \begin{cases} -\nabla \cdot (u \nabla \mu) + g \rho v \mu + j\omega \lambda = 0 & \text{on } \Gamma_c \\ \mu_n = 0 & \text{on } \partial \Gamma_c \end{cases} \\ \text{Control:} \quad & \begin{cases} \mathcal{L}'_u[\psi - u^*] = \int_{\Gamma_c} \beta_u \nabla u^* \cdot \nabla (\psi - u^*) \\ \quad + [\alpha_u u^* + \Re(\nabla \bar{\mu}^* \cdot \nabla \eta^*)](\psi - u^*) \geq 0 & \forall \psi \in \mathcal{U}_{ad} \\ \mathcal{L}'_v[\psi - v^*] = \int_{\Gamma_c} \beta_v \nabla v^* \cdot \nabla (\psi - v^*) \\ \quad + [\alpha_v v^* + g \rho \Re(\bar{\mu}^* \eta^*)](\psi - v^*) \geq 0 & \forall \psi \in \mathcal{V}_{ad} \end{cases} \end{aligned} \quad (48)$$

where $(\phi^*, \lambda^*, \eta^*, \mu^*, u^*, v^*)$ is the optimal solution of the control problem.

Note that this is a nonlinear OCP, thus the solution must be obtained by means of an iterative approach.

Relying on the same discretization as before, we obtain the following optimality conditions

$$\begin{aligned} \text{States:} \quad & \begin{cases} \left[A - \frac{\omega^2}{g} C_f + \alpha C_c \right] \phi = j\omega K_g^\top \{\mathbf{X}\} + j\omega D_c \eta + \mathbf{f}_g + \mathbf{f}_c \\ (K - \omega^2 M) \{\mathbf{X}\} = -j\omega \rho (K_g \phi + \mathbf{g}) \\ (\mathbf{A} \mathbf{u} + \rho g \mathbb{B} \mathbf{v}) \eta = -j\omega \rho D_c^\top \phi \end{cases} \\ \text{Adjoint states:} \quad & \begin{cases} \left[A - \frac{\omega^2}{g} C_f + \bar{\alpha} C_c \right] \lambda = j\omega \rho K_g^\top \{\mathbf{Y}\} + j\omega \rho D_c \mu \\ (K - \omega^2 M)^\top \{\mathbf{Y}\} = -j\omega K_g \lambda - C^\top \{\mathbf{X}\} \\ (\mathbf{A} \mathbf{u} + \rho g \mathbb{B} \mathbf{v}) \mu = -j\omega D_c^\top \phi \end{cases} \\ \text{Control gradients:} \quad & \begin{cases} \nabla_u J = (\alpha_u E_c + \beta_u A_c) \mathbf{u} + \Re(\bar{\mu} \mathbb{A} \eta) \\ \nabla_v J = (\alpha_v E_c + \beta_v A_c) \mathbf{v} + g \rho \Re(\bar{\mu} \mathbb{B} \eta) \end{cases} \end{aligned} \quad (50)$$

where the third order tensors $\mathbb{A}, \mathbb{B} \in \mathbb{R}^{n \times n \times l}$ are defined as

$$(\mathbb{A})_{ijk} := \int_{\Gamma_c} \nabla \phi_i \cdot \nabla \phi_j \psi_k d\Gamma, \quad (\mathbb{B})_{ijk} := \int_{\Gamma_c} \phi_i \phi_j \psi_k d\Gamma, \quad (51)$$

and the products $\mathbf{A} \mathbf{u}$ and $\mu \mathbb{A}$ are matrices defined as

$$(\mathbf{A} \mathbf{u})_{ij} := \sum_{k=1}^l (\mathbb{A})_{ijk} u_k, \quad (\mu \mathbb{A})_{kj} := \sum_{i=1}^n \mu_i (\mathbb{A})_{ijk}. \quad (52)$$

We consider the same setup adopted for the pressure-controlled case, but a model of the floating membrane is added on the surface Γ_c . We set $\alpha_u = \alpha_v = 1 \times 10^{-4}$ and $\beta_u = \beta_v = 4 \times 10^{-2}$; then, we solve the nonlinear OCP relying on the Matlab[®] interface for IPOPT by Wächter and Biegler (2006), Bertolazzi (2022), a software package for large-scale nonlinear optimization. The resulting optimal T and m are shown in Fig. 3 along with the optimization convergence in terms of cost minimization. Note that the wave speed increases according to T and inversely to m , and the wave is steered due to their gradient leading to a refraction effect (Keller and Goldstein, 1953). The results show that only the mass has strong fluctuations; this in turn suggests that the wave is steered by local resonances of the membrane. Anyway, by comparing Figs. 3(a) and 3(b), one can appreciate the complementary role of T and m : whereas the mass assumes high values, the stiffness is low and vice versa.

5. Floating plate

The control strategy just proposed seems effective on reducing the floating body motion; however a device with variable surface tension can be of difficult realization due to the problems of internal equilibrium discussed above, then a more sophisticated control can be useful

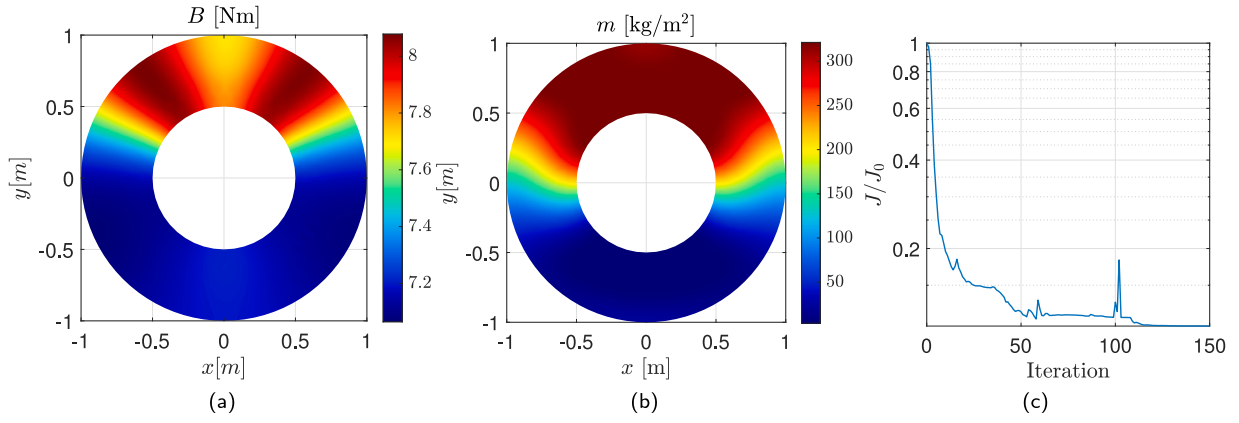


Fig. 4. Plate properties given by the optimal control: flexural modulus B (a) and surface mass density m (b); objective over iteration (c). The improvement of the oscillations $\{\mathbf{X}\}$ is summarized in Table 1. The slow fluctuations in both stiffness and mass show that the water wave is not steered around the sphere but it is mostly attenuated by the plate resonance.

in practice. In particular, the elastic restoring force given by surface tension must be replaced by another one.

Through this section, the control surface Γ_c is loaded by a floating elastic thin plate. The model we adopt is similar to the one proposed in the literature for studying the effect of floating ice on water waves, see e.g. Balmforth and Craster (1999), Fox and Squire (1990). In this setting, the plate stiffness acts as a restoring force thus increasing the wave speed, conversely, the load inertia slows it down. So, similarly to the previous case, we expect to control the water flow by deriving stiffness and inertia properties of the plate.

Let us consider the plate equilibrium in weak form (Timoshenko et al., 1959):

$$\int_{\Gamma_c} B[(1-\nu)D^2\eta : D^2v + \nu\Delta\eta\Delta v] d\Gamma = \int_{\Gamma_c} f v d\Gamma \quad \forall v \in \mathcal{Y}, \quad (53)$$

where $B : \Gamma_c \rightarrow \mathbb{R}$ is the local flexural stiffness, ν is the Poisson ratio of the plate material, f is a distributed load pointing upwards. $D^2\eta$ is the hessian matrix of η and $A : B$ indicates the Frobenius scalar product between matrices A and B , i.e. $A : B := \sum_{i,j=1}^2 (A)_{ij}(B)_{ij}$. Note that in this case, we need to require that $\eta \in \mathcal{Y} = H^2(\Gamma_c)$ for a correct definition of the weak formulation (53). By following a procedure similar to the one in Timoshenko et al. (1959), we can derive the strong form in the case of space dependent B :

$$\begin{cases} \Delta(B\Delta\eta) + (1-\nu)(2B_{xy}\eta_{xy} - B_{xx}\eta_{yy} - B_{yy}\eta_{xx}) - f = 0 & \text{in } \Gamma_c \\ \Delta\eta - (1-\nu)\eta_{\tau\tau} = 0 & \text{on } \partial\Gamma_c \\ (B\Delta\eta)_n + (1-\nu)(2B_\tau\eta_{n\tau} - B_n\eta_{n\tau} + B\eta_{n\tau\tau}) = 0 & \text{on } \partial\Gamma_c \end{cases} \quad (54)$$

where the subscript τ stands for the tangential derivative on the boundary. Note that the two conditions on $\partial\Gamma_c$ hold because we impose the plate edges to be free, i.e. null torque and null shear. The force f acting on the plate is given by the inertia of the plate itself and the water pressure obtained from Eq. (5), then

$$f = -m\zeta_{tt} - mg - \rho g\zeta - \rho\Phi_t, \quad (55)$$

and, in the frequency domain,

$$f = (m\omega^2 - \rho g)\eta - j\omega\rho\phi. \quad (56)$$

The control problem reads: find u, v that minimize Eq. (46) where the three coupled dynamics, (21) and (54) are satisfied, with $u \in \mathcal{U}_{ad}$, $v \in \mathcal{V}_{ad}$ where

$$B = u \quad 1 - \frac{\omega^2 m}{g\rho} = v; \quad (57)$$

and $\mathcal{U}_{ad}, \mathcal{V}_{ad}$ are defined by Eq. (45). Again, we apply the Lagrange's multipliers method for obtaining the first order necessary conditions,

similarly to Eq. (47) we define $\mathcal{N} : \mathcal{W} \times \mathcal{W}' \times \mathbb{C}^6 \times \mathbb{C}^6 \times \mathcal{Y} \times \mathcal{Y}' \times \mathcal{U} \times \mathcal{U}' \rightarrow \mathbb{R}$ as

$$\begin{aligned} \mathcal{N}(\phi^s, \lambda, \{\mathbf{X}\}, \{\mathbf{Y}\}, \eta, \mu, u, v) := & J + \Re \left\{ \int_{\Omega} \nabla \bar{\lambda} \cdot \nabla \phi^s \right. \\ & - \frac{\omega^2}{g} \int_{\Gamma_f} \bar{\lambda} \phi^s + \int_{\Gamma_c} \bar{\lambda}(\phi_n^i - j\omega\eta) \\ & - j\omega \int_{\Gamma_g} \bar{\lambda} \{\mathbf{n}\}^\dagger \{\mathbf{X}\} + \int_{\Gamma_g} \bar{\lambda} \phi_n^i + \alpha \int_{\Gamma_e} \bar{\lambda} \phi^s \\ & \left. + \{\mathbf{Y}\}^\dagger \left[(K - \omega^2 M) \{\mathbf{X}\} + j\omega\rho \int_{\Gamma_g} (\phi^s + \phi^i) \{\mathbf{n}\} \right] \right\} \\ & + \int_{\Gamma_c} u \left[(1-\nu)D^2\eta : D^2\bar{\mu} + \nu\Delta\eta\Delta\bar{\mu} \right] + \int_{\Gamma_c} [g\rho v\eta + j\omega\rho(\phi^s + \phi^i)]\bar{\mu} \}. \quad (58) \end{aligned}$$

Following the same procedure as before, we obtain the adjoints equations in the strong form

$$\begin{cases} -\Delta\lambda = 0 & \text{in } \omega \\ \lambda_n = 0 & \text{on } \Gamma_r \\ \lambda_n - \frac{\omega^2}{g}\lambda = 0 & \text{on } \Gamma_f \\ \lambda_n = j\omega\rho\mu & \text{on } \Gamma_c \\ \lambda_n = j\omega\rho\{\mathbf{n}\}^\dagger \{\mathbf{Y}\} & \text{on } \Gamma_g \\ \lambda_n + \bar{\alpha}\lambda = 0 & \text{on } \Gamma_e \end{cases}$$

$$(K - \omega^2 M)^\dagger \{\mathbf{Y}\} = -j\omega \int_{\Gamma_g} \lambda \{\mathbf{n}\} d\Gamma - C^\dagger \{\mathbf{X}\}$$

$$\begin{cases} \Delta(u\Delta\mu) + (1-\nu)(2u_{xy}\mu_{xy} - u_{xx}\mu_{yy} - u_{yy}\mu_{xx}) + \rho g v\mu + j\omega\lambda = 0 & \text{in } \Gamma_c \\ \Delta\mu - (1-\nu)\mu_{\tau\tau} = 0 & \text{on } \partial\Gamma_c \\ (u\Delta\mu)_n + (1-\nu)(2u_\tau\mu_{n\tau} - u_n\mu_{n\tau} + u\mu_{n\tau\tau}) = 0 & \text{on } \partial\Gamma_c \end{cases} \quad (59)$$

and the control gradients

$$\begin{aligned} \mathcal{L}'_u[\psi - u^*] = & \int_{\Gamma_c} \beta_u \nabla u^* \cdot \nabla(\psi - u^*) + [\alpha_u u^* + \Re(\nabla \bar{\mu}^* \cdot \nabla \eta^*)](\psi - u^*) \geq 0 \\ & \forall \psi \in \mathcal{U}_{ad} \\ \mathcal{L}'_v[\psi - v^*] = & \int_{\Gamma_c} \beta_v \nabla v^* \cdot \nabla(\psi - v^*) + [\alpha_v v^* + g\rho \Re(\bar{\mu}^* \eta^*)](\psi - v^*) \geq 0 \\ & \forall \psi \in \mathcal{V}_{ad} \end{aligned} \quad (60)$$

Finally, the first order optimality conditions are discretized in order to obtain a numerical solution. With respect to the discrete nonlinear

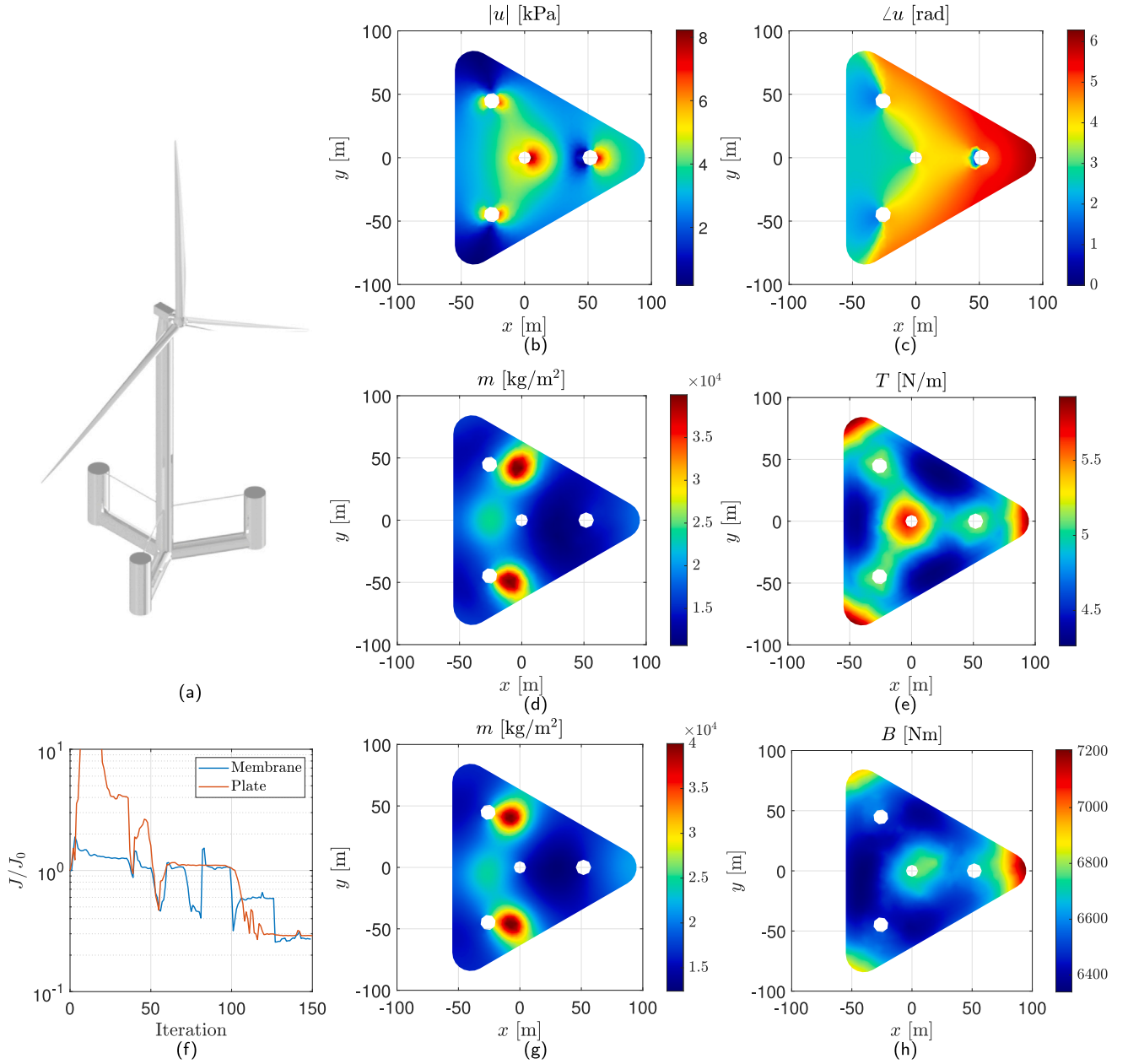


Fig. 5. (a) The shape of the floating wind turbine VoltornUS-S considered in the study. (b) and (c) show respectively amplitude and phase of the pressure applied; (d) and (e) surface mass and tension of the membrane; (f) costs over iterations for the cases of membrane and plate control; (g) and (h) surface mass and flexural stiffness of the plate. Note that the mass concentrates in very similar places for membrane (d) and plate (g) controllers; also, the stiffness properties in (e) and in (h) show high values on similar zones of the control surface. This suggests which zones are the most effective for placing the control mechanism..

system (50), the only difference we have is that the stiffness tensor \mathbb{A} , describing the elastic restoring force due to internal tension, is substituted by \mathbb{L} that accounts for the flexural stiffness. For this reason, we do not rewrite the entire set of equations. However, it is important to highlight how \mathbb{L} is defined, that is

$$(\mathbb{L})_{ijk} := \int_{\Gamma_c} \psi_k [(1-\nu) D^2 \phi_i : D^2 \phi_j + \nu \Delta \phi_i \Delta \phi_j] d\Gamma, \quad (61)$$

that is numerical consistent only if $\mathcal{W}_h \subseteq H^2(\Omega)$, which is not the case for a FEM based on \mathbb{P}_1 shape functions. In order to overcome this issue while avoiding the computational effort required by standard

nonconforming or mixed methods (Joly et al., 2005), we adopt the recovery gradient technique described in Guo et al. (2018) that allows to solve biharmonic problems relying on C^0 finite elements.

The setup studied before is now controlled by means of a plate whose properties are determined by solving the corresponding nonlinear OCP. Again, the minimization is carried out by making use of IPOPT software; the results in terms of optimal stiffness and inertia properties are shown in Fig. 4 and the vibration reductions are highlighted in Table 1. Similarly to the membrane, the roles of stiffness B and mass m are, respectively, to accelerate and decelerate the wave speed (Fox and Squire, 1990); this, in turn, steers the wave propagation by refraction.

Table 2

Comparison between the turbine motion for the three different control strategies; the value describing rotation about z-axis is not reported because it is almost zero in every case and derives from numerical errors only. High performance is reached with all three strategies, but a fair comparison should consider the actual possibility to realize the control mechanisms.

{X} [m/° < rad]	Uncontrolled	Pressure-controlled	Membrane-controlled	Plate-controlled
x	0.613 < -1.63	0.292 < -1.63	0.056 < -1.87	0.055 < -1.38
y	0.000 < -2.35	0.000 < -1.53	0.053 < 1.61	0.012 < 1.59
z	0.708 < -3.11	0.121 < -3.10	0.070 < -1.86	0.057 < -0.36
θ_x	0.000 < -4.68	0.000 < -3.81	0.221 < -3.61	0.148 < 2.72
θ_y	0.103 < -4.27	0.015 < -3.29	1.706 < -2.96	0.484 < 3.39
J	4.38×10^{-1}	2.14×10^{-1}	1.81	1.82
$\frac{1}{2} \{X\}^T C \{X\}$	4.38×10^{-1}	5.00×10^{-2}	5.86×10^{-3}	3.22×10^{-3}

The solution shows slow fluctuations of both stiffness and mass, so we can conclude that the waves are attenuated by a distributed resonance of the plate and the refraction effect is small.

6. Floating wind turbine

In the following, we apply the three control strategies to the semi-submersible floating wind turbine depicted in 5, which is a standard defined by the European project (IEAWindTask37, 2023). The geometry and the mass parameters are computed according to the reference, so the stiffness and mass matrices K and M are defined by Eq. (16). The non-null eigenvalues of $M^{-1}K$ approximate the resonances of the floating structures, that correspond to the time periods of $T_1 = 13.47$ s for heave motion, $T_2 = 36.33$ s for pitch and $T_3 = 36.30$ s for roll. By selecting the excitation period to be 13 s, the system is excited about resonance at $\omega = 0.48 \text{ rad s}^{-1}$. The seabed is set to be 100 m deep, the wave comes from left, and the regularization parameters are set as $\alpha_u = \alpha_v = 1 \times 10^{-4}$, $\beta_u = \beta_v = 1 \times 10^{-1}$ for both the membrane and plate control problems.

Figures from 5b to 5h show the control actions applied and in Table 2 one can appreciate the oscillation reduction in terms of amplitude, phase, and minima of the cost functionals according to the three problems defined above (see Fig. 5).

7. Conclusions

In this work, we introduced a control-theoretic framework to modify the interaction between water waves and floating objects by acting on their surroundings through both active and passive control mechanisms. The active control consists of applying pressure which is optimally modulated in space to reduce the target's motion. The resulting OCP is linear-quadratic and it is solved efficiently with a *one-shot* approach. This active mechanism greatly reduces the oscillations but it may be difficult to realize in practice. As a consequence, we introduced two passive control mechanisms which are themselves floating objects with tunable properties, a membrane, and a thin plate. By optimally modulating in space their physical properties, we showed how these mechanisms can still reduce the oscillations by two and one order of magnitudes, respectively. The control problem is bilinear in both cases and a system of first-order optimality conditions is derived using variational calculus. The resulting system is then solved iteratively.

On one hand, the results in this paper pave the way for a general and rigorous vibration control strategy which also provides effective design guidelines for reducing hydrodynamic excitation on arbitrary objects. On the other hand, the framework we introduced is rather general and several other problems, such as cloaking, energy harvesting, etc., can be solved by properly modifying the cost functional.

Future work focuses on the design of the specific actuators and devices needed, along with analysis of the achievable limits on their physical properties. Such limits could be easily included into the optimization algorithm as constraints in the formulation of the problem.

CRediT authorship contribution statement

Sebastiano Cominelli: Formal analysis, Software, Validation, Visualization, Writing. **Carlo Sinigaglia:** Conceptualization, Methodology, Writing. **Davide Enrico Quadrelli:** Conceptualization, Writing. **Francesco Braghin:** Supervision, Project administration.

Declaration of competing interest

The authors declare that they have no known competing financial interests or personal relationships that could have appeared to influence the work reported in this paper.

Data availability

Data will be made available on request.

References

- Adedipe, O., Brennan, F., Kolios, A., 2016. Review of corrosion fatigue in offshore structures: Present status and challenges in the offshore wind sector. *Renew. Sustain. Energy Rev.* 61, 141–154.
- Alam, M.R., 2012. Broadband cloaking in stratified seas. *Phys. Rev. Lett.* 108 (8), 084502.
- Bai, K.J., 1972. A Variational Method in Potential Flows with a Free Surface. Technical Report, California University Berkeley College of Engineering.
- Balmforth, N., Craster, R., 1999. Ocean waves and ice sheets. *J. Fluid Mech.* 395, 89–124.
- Bertolazzi, E., 2022. mexIPOPT. <https://github.com/ebertolazzi/mexIPOPT>. (Accessed 23 March 2022).
- Colwell, S., Basu, B., 2009. Tuned liquid column dampers in offshore wind turbines for structural control. *Eng. Struct.* 31 (2), 358–368.
- Cominelli, S., Quadrelli, D.E., Sinigaglia, C., Braghin, F., 2022. Design of arbitrarily shaped acoustic cloaks through partial differential equation-constrained optimization satisfying sonic-metamaterial design requirements. *Proc. R. Soc. Lond. Ser. A Math. Phys. Eng. Sci.* 478 (2257), 20210750.
- Cummer, S.A., Schurig, D., 2007. One path to acoustic cloaking. *New J. Phys.* 9 (3), 45.
- Dupont, G., Guenneau, S., Kimmoun, O., Molin, B., Enoch, S., 2016. Cloaking a vertical cylinder via homogenization in the mild-slope equation. *J. Fluid Mech.* 796.
- Farhat, M., Enoch, S., Guenneau, S., Movchan, A., 2008. Broadband cylindrical acoustic cloak for linear surface waves in a fluid. *Phys. Rev. Lett.* 101 (13), 134501.
- Fox, C., Squire, V.A., 1990. Reflection and transmission characteristics at the edge of shore fast sea ice. *J. Geophys. Res.: Oceans* 95 (C7), 11629–11639.
- Guo, H., Zhang, Z., Zou, Q., 2018. A C^0 linear finite element method for biharmonic problems. *J. Sci. Comput.* 74 (3), 1397–1422.
- Hasselmann, K., Barnett, T.P., Bouws, E., Carlson, H., Cartwright, D.E., Enke, K., Ewing, J., Gienapp, A., Hasselmann, D., Kruseman, P., et al., 1973. Measurements of wind-wave growth and swell decay during the joint north sea wave project (JONSWAP). *Ergaenzungsheft Zur Deutschen Hydrogr. Zeitschrift, Reihe A*.
- Hsu, T.W., Lan, Y.J., Tsay, T.K., Lin, K.P., 2003. Second-order radiation boundary condition for water wave simulation with large angle incidence. *J. Eng. Mech.* 129 (12), 1429–1438.
- IEAWindTask37, 2023. IeaWindTask37. <https://github.com/IEAWindTask37>. (Accessed 05 March 2023).
- Iida, T., Zareei, A., Alam, M.R., 2023. Water wave cloaking using a floating composite plate. *J. Fluid Mech.* 954, A4.
- Jahangiri, V., Sun, C., 2020. Three-dimensional vibration control of offshore floating wind turbines using multiple tuned mass dampers. *Ocean Eng.* 206, 107196.

- Joly, P., Quarteroni, A., Rappaz, J., 2005. *Scientific Computation*. Springer.
- Kadic, M., Schittny, R., Bückmann, T., Wegener, M., 2016. Experiments on cloaking in electromagnetism, mechanics, and thermodynamics. *Transform. Wave Phys.: Electromagn., Elastodyn. Thermodyn.* 335–368. <http://dx.doi.org/10.1201/9781315364742>.
- Kandasamy, R., Cui, F., Townsend, N., Foo, C.C., Guo, J., Shenoi, A., Xiong, Y., 2016. A review of vibration control methods for marine offshore structures. *Ocean Eng.* 127, 279–297.
- Keller, J.B., Goldstein, E., 1953. Water wave reflection due to surface tension and floating ice. *EOS Trans. Am. Geophys. Union* 34 (1), 43–48.
- Leonhardt, U., 2006. Optical conformal mapping. *Science* 312 (5781), 1777–1780.
- Loukogeorgaki, E., Kashiwagi, M., 2019. Minimization of drift force on a floating cylinder by optimizing the flexural rigidity of a concentric annular plate. *Appl. Ocean Res.* 85, 136–150.
- Manzoni, A., Quarteroni, A., Salsa, S., 2021. *Optimal Control of Partial Differential Equations*. Springer.
- Mei, C.C., Stiassnie, M.A., Yue, D.K.-P., 2005. *Theory and Applications of Ocean Surface Waves: Part 1: Linear Aspects*. World Scientific.
- Negri, F., 2016. *RedbKIT version 2.2*. <http://redbkit.github.io/redbKIT/>.
- Newman, J., 2014. Cloaking a circular cylinder in water waves. *Eur. J. Mech. B Fluids* 47, 145–150.
- Norris, A.N., Shuvalov, A.L., 2011. Elastic cloaking theory. *Wave Motion* 48 (6), 525–538.
- Pendry, J.B., Schurig, D., Smith, D.R., 2006. Controlling electromagnetic fields. *Science* 312 (5781), 1780–1782.
- Porter, R., Newman, J., 2014. Cloaking of a vertical cylinder in waves using variable bathymetry. *J. Fluid Mech.* 750, 124–143.
- Schittny, R., Kadic, M., Guenneau, S., Wegener, M., 2013. Experiments on transformation thermodynamics: Molding the flow of heat. *Phys. Rev. Lett.* 110 (19), 195901.
- Sinigaglia, C., Quadrelli, D.E., Manzoni, A., Braghin, F., 2022. Fast active thermal cloaking through PDE-constrained optimization and reduced-order modelling. *Proc. R. Soc. Lond. Ser. A Math. Phys. Eng. Sci.* 478 (2258), 20210813.
- Timoshenko, S., Woinowsky-Krieger, S., et al., 1959. *Theory of Plates and Shells*, Vol. 2. McGraw-hill New York.
- Wächter, A., Biegler, L.T., 2006. On the implementation of an interior-point filter line-search algorithm for large-scale nonlinear programming. *Math. Program.* 106 (1), 25–57.
- Wirtinger, W., 1927. Zur formalen theorie der funktionen von mehr komplexen veränderlichen. *Math. Ann.* 97 (1), 357–375.
- Zareei, A., Alam, M.R., 2015. Cloaking in shallow-water waves via nonlinear medium transformation. *J. Fluid Mech.* 778, 273–287.
- Zareei, A., Alam, R., 2016. Cloaking by a floating thin plate. In: *Proc. 31st Int. Workshop on Water Waves and Floating Bodies*. Michigan, USA, pp. 197–200.
- Zhang, Z., He, G., Kashiwagi, M., Wang, Z., 2018. A quasi-cloaking phenomenon to reduce the wave drift force on an array of adjacent floating bodies. *Appl. Ocean Res.* 71, 1–10.
- Zhang, Z., He, G., Wang, W., Liu, S., Wang, Z., 2020. Reduction of wave drift force on a truncated cylinder in a wide frequency band using the defect effects on cloaking phenomenon. *Ocean Eng.* 203, 107241.
- Zuo, H., Bi, K., Hao, H., 2020. A state-of-the-art review on the vibration mitigation of wind turbines. *Renew. Sustain. Energy Rev.* 121, 109710.